

Structural investigations of a neutralized polyelectrolyte gel and an associating neutral hydrogel

Ferenc Horkay^{a,*}, Peter J. Basser^a, Anne-Marie Hecht^b, Erik Geissler^b

^aSection on Tissue Biophysics and Biomimetics, Laboratory of Integrative and Medical Biophysics, NICHD, National Institutes of Health, 13 South Drive, Bethesda, MD 20892, USA

^bLaboratoire de Spectrométrie Physique CNRS UMR 5588, Université J. Fourier de Grenoble, B.P.87, 38402 St Martin d'Hères, France

Available online 11 March 2005

Dedicated to Professor James E. Mark on the occasion of his 70th birthday.

Abstract

Small angle neutron scattering (SANS) measurements are used to differentiate the local organization of the polymer chains in two different classes of hydrogel. In neutral polyvinyl alcohol gels, hydrogen bonding gives rise to long range structural perturbations that are superimposed on the underlying chemically cross-linked network, thus producing excess scattering at small values of the scattering vector q . This secondary superstructure causes an increase in the elastic modulus. The intensity scattered by the thermal fluctuations in these gels can be described by an Ornstein–Zernike lineshape and is consistent with the osmotic modulus deduced from macroscopic osmotic and mechanical observations.

Strongly charged polyacrylate hydrogels, however, display a qualitatively different scattering response. At low q a power law behavior is observed characteristic of a fractal surface. At intermediate q another component of osmotic origin is visible, which varies as q^{-1} , which indicates that the presence of divalent cations favors linear alignment of the network chains. Acceptable agreement is found between the estimate of the thermal fluctuations deduced from SANS and the results derived from independent osmotic observations.

© 2005 Elsevier Ltd. All rights reserved.

Keywords: Hydrogel; Polyelectrolyte; Small angle neutron scattering

1. Introduction

A large body of experimental work has been devoted to the understanding of the structure and macroscopic mechanical and swelling properties of neutral polymer gels [1–5]. In the absence of interactions the elementary building blocks consist of Gaussian coils. In the presence of excluded volume interactions, the coil expands. In addition, however, when the individual chains are connected in a continuous network, local elastic constraints are incorporated that generate random permanent concentration variations when the gel is swollen.

Only a few investigations in which both structural and

macroscopic mechanical and osmotic measurements were simultaneously made have been reported for gels where hydrogen bonding or long range Coulomb forces dominate [5,6]. It is known that these interactions give rise to a complex hierarchy of structures each defined by a different characteristic length scale. Hydrogen bonding and hydration play a key role in stabilizing the structure of biopolymers. Electrostatic interactions between free ions and those bound to the polymer chain are also important in almost all biological systems. Although several studies have been devoted to weakly charged polyelectrolyte gels [6–8], no systematic investigations have been undertaken into strongly charged polyelectrolyte gels in the presence of excess salt [9]. In what follows, we briefly review some of our previous findings and present new experimental results.

The goal of this article is to investigate the effects of hydrogen bonding and the presence of charged groups on the structure and thermodynamic properties of swollen cross-linked polymer networks. The effect of hydrogen bonding is illustrated on polyvinyl alcohol gels. Sodium polyacrylate is used to study the effect of divalent ions on

* Corresponding author. Address: Bldg. 13, Room 3W16E, National Institutes of Health, 13 South Drive, Bethesda, MD 20892, USA. Tel.: +1 301 435-7229; fax: +1 301 435-5035.

E-mail address: horkay@helix.nih.gov (F. Horkay).

the structure and osmotic properties of a polyelectrolyte. In the latter, the ionic composition and concentration is varied by addition of calcium chloride to gels equilibrated with nearly physiological sodium chloride solutions. Small angle neutron scattering (SANS) is used to investigate the structural changes, while osmotic swelling pressure measurements are made to determine the thermodynamic interactions. Furthermore, the behavior of sodium polyacrylate gels is compared with that of the corresponding neutral hydrogel polyacrylamide.

2. Theoretical considerations

2.1. SANS in polymer gels

For gels composed of flexible polymer coils the scattering intensity can usually be described by a sum of a dynamic and a static component [3–5]

$$I(q) = I_{\text{osm}}(q) + I_x(q) \quad (1)$$

in which

$$I_{\text{osm}}(q) = \Delta\rho^2 \frac{kT\varphi^2}{\varphi\partial\omega/\partial\varphi + 4G/3} \frac{1}{1 + q^2\xi^2} \quad (2)$$

here $\Delta\rho^2$ is the contrast factor between the solvent and the polymer, k is the Boltzmann constant and ξ is the thermal correlation length. $I_x(q)$ is the contribution of the frozen-in structural features, φ is the polymer volume fraction, ω the osmotic swelling pressure of the cross-linked polymer and G is the shear modulus. The amplitude of the scattering vector q is given by

$$q = (4\pi/\lambda)\sin(\theta/2) \quad (3)$$

where λ is the wavelength of the incident neutrons and θ is the scattering angle. In Eq. (2), the denominator of the first term is the longitudinal osmotic modulus of the gel, which can also be determined independently from osmotic and mechanical measurements. For neutral gels it is usually found that concentration fluctuations frozen-in by the cross-links cause extra scattering $I_x(q)$, which is described by a Debye–Bueche structure factor [10]

$$I_x(q) = \Delta\rho^2 \frac{8\pi\Xi^3\langle\delta\varphi^2\rangle}{(1 + q^2\Xi^2)^2} \quad (4)$$

where Ξ is the correlation length of the frozen-in structure and $\langle\delta\varphi^2\rangle$ is the mean square amplitude of the associated concentration fluctuations. In systems containing additional superstructures, such as aggregated domains or crystallites, $I_x(q)$ includes further terms, the functional form of which depends on the nature of the association.

2.2. Thermodynamics of polymer gels

The swelling pressure of a neutral polymer gel ω is given

by:

$$\omega = \Pi - G \quad (5)$$

The mixing contribution Π can be expressed as [11]

$$\Pi = -(RT/v_1)[\ln(1 - \varphi) + \varphi + \chi_0\varphi^2 + \chi_1\varphi^3] \quad (6)$$

where v_1 is the molar volume of the solvent, R is the gas constant, T the absolute temperature, and χ_0 and χ_1 are constants. Thus the longitudinal osmotic modulus M_{os} governing the scattering properties of the gel, is then [12]

$$M_{\text{os}} = \varphi\partial\omega/\partial\varphi + 4G/3 \\ = \varphi^2(RT/v_1)\{1/(1 - \varphi) - 2\chi_0 - 3\chi_1\varphi\} + G \quad (7)$$

According to the theory of rubber elasticity [13], the elastic modulus is given by

$$G = G_0\varphi^m \quad (8)$$

where G_0 is a constant and the exponent $m = 1/3$.

3. Experimental methods

3.1. Gel preparation

The preparation of polyacrylamide (PAA) and sodium polyacrylate (PSA) gels has been described previously [4,9]. These gels were synthesized by free-radical copolymerization from their respective monomers and the cross-linker N,N' -methylenebis(acrylamide) in aqueous solution. Ammonium persulfate was used as an initiator. In both systems, the concentration of the cross-linker was 0.3%. After gelation the PAA gel was washed and then swollen in deionized water. In the PSA gels the acrylic acid units were first neutralized in NaOH and equilibrated with aqueous solutions of 40 mM NaCl. Then the concentration of CaCl_2 in the equilibrium solution was increased gradually up to 0.8 mM CaCl_2 . At CaCl_2 concentrations higher than 1 mM a volume transition occurs in this system [9]. SANS measurements were made both below and above this concentration.

Poly(vinyl-alcohol) (PVA) gels were made by cross-linking with glutaraldehyde at pH = 1.5 in aqueous solutions [5]. For the experiments fractionated polymer samples were used ($M_w^{\text{PVA}} = 110,000$). Cross-links were introduced at polymer concentration 5% (w/w), the molar ratio of monomer units to the molecules of cross-linker was 400.

3.2. Small angle neutron scattering measurements

SANS measurements were performed at the Institut Laue Langevin (ILL), Grenoble, France and also at NIST, Gaithersburg MD [14]. At the ILL the D22 instrument was used with an incident wavelength of 8 Å. The sample-detector distances were 2, 6 and 18 m, corresponding to an explored wave vector range $0.002 \text{ \AA}^{-1} \leq q \leq 0.15 \text{ \AA}^{-1}$. The

ambient temperature during the experiments was $25^\circ \pm 0.1^\circ \text{C}$. Gel samples were prepared in solutions of heavy water in 2 mm thick sample cells. At NIST, the measurements were made on the NG3 instrument at two sample-detector distances, 2.5 and 13.1 m, with incident wavelength 8 Å. After azimuthal averaging, corrections for incoherent background, detector response and cell window scattering were applied.

3.3. Light scattering measurements

Static light scattering measurements were made in the angular range $30\text{--}150^\circ$ using an ALV/SP-86 automatic goniometer (ALV, Langen, Germany), together with a Spectra Physics 2020 Krypton ion laser working at 647.1 nm. Dynamic light scattering measurements were made by an ALV-3000 multibit correlator (ALV, Langen, FRG).

The absolute intensity was calibrated using pure toluene. The measurements were made at $25 \pm 0.1^\circ \text{C}$. The coherence factor of the optical detection was $\beta = 0.93 \pm 0.02$.

3.4. Osmotic and mechanical measurements

Gels were equilibrated with poly(vinyl pyrrolidone) solutions (molecular weight: 29 kDa) of known osmotic pressure [15,16]. A semi-permeable membrane was used to prevent penetration of the polymer into the network. When equilibrium was reached, the concentration of both phases was measured. This procedure gives for each gel the dependence of ω upon the polymer volume fraction, ϕ .

The shear modulus of the gels was determined using a TA.XT2I HR Texture Analyser (Stable Micro Systems, UK). The measurements were performed under uniaxial compression on cylindrical specimens in equilibrium with the salt solutions at deformation ratios $0.7 < \lambda < 1$. The shear modulus, G , was calculated from the nominal stress, σ (force per unit undeformed cross-section), using the relation [13]

$$\sigma = G(\lambda - \lambda^{-2}) \quad (9)$$

The absence of volume change and barrel distortion during these measurements was verified. All measurements were carried out at $25 \pm 0.1^\circ \text{C}$.

4. Results and discussion

4.1. Neutral hydrogels

Fig. 1 shows the typical scattering response for a highly swollen neutral gel (polyacrylamide). To extend the range of wave vectors q , data obtained from static light scattering (SLS) are also shown, expressed in terms of the same absolute units as the SANS measurements. For the SLS

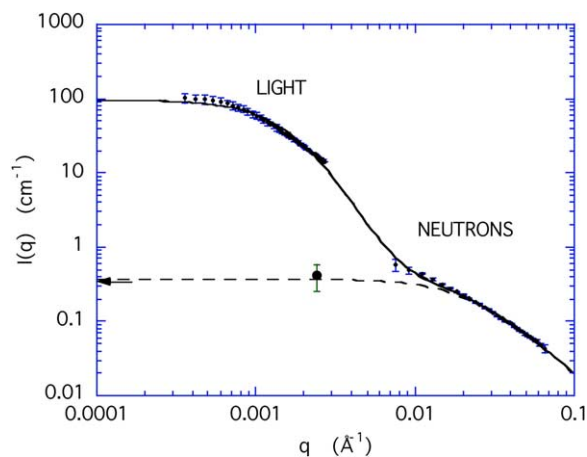


Fig. 1. Combined SANS and SLS spectra from polyacrylamide hydrogel at polymer concentration $\phi = 0.05$ with cross-link density 0.3%. Correlation lengths from the fit to Eq. (1) are $\xi = 43 \text{ \AA}$ and $\Xi = 390 \text{ \AA}$. Dashed line: first term of Eq. (1). Horizontal arrow: intensity estimated from macroscopic osmotic swelling pressure measurements (Eq. (7)) together with the corresponding neutron scattering contrast factor. Filled circle: intensity of osmotic fluctuations determined by DLS.

measurements the gel was rotated in order to yield an ensemble average over the speckle pattern scattered by the sample [17]. Two plateaus can be seen, one in the intermediate q region and the other at low q . At high q a shoulder is visible, which corresponds to the Ornstein–Zernike thermal contribution to the scattering [18,19]. At lower q the excess scattering can be attributed to elastic constraints, as well as to clusters of the cross-linker, and is described by Eq. (4). The dashed curve in Fig. 1 is the calculated thermal component of the fit, while the arrow at the ordinate axis of this figure gives the intensity calculated from the swelling pressure measurements and the corresponding neutron contrast factor [20] for this system ($\Delta\rho^2 = 1.81 \times 10^{29} \text{ m}^{-4}$). The data point at $q = 0.0024 \text{ \AA}^{-1}$ (scattering angle 90°) is the intensity of the temporal fluctuations measured by dynamic light scattering (DLS) [17], expressed in the same neutron scattering units. Within the experimental uncertainties of these three independent techniques, these results are in acceptable agreement.

A second example of a neutral gel is shown in Fig. 2 where the scattering response of polyvinyl alcohol (PVA) hydrogel is displayed. As in Fig. 1, the continuous line is the fit of the SANS data points to Eq. (1), the thermal component of which is represented by the dashed line. These data are in agreement with both the DLS results (squares) and the numerical value deduced from the swelling pressure measurements (arrow at left of figure).

It is known that in PVA solutions microcrystallites are present, as a consequence of hydrogen bonding. These objects also contribute to the excess scattering intensity, since not only do the microcrystallite nuclei produce scattering but also they generate an elastic strain field around them, which modifies the local polymer concentration. The light scattering region of Fig. 2 indicates the

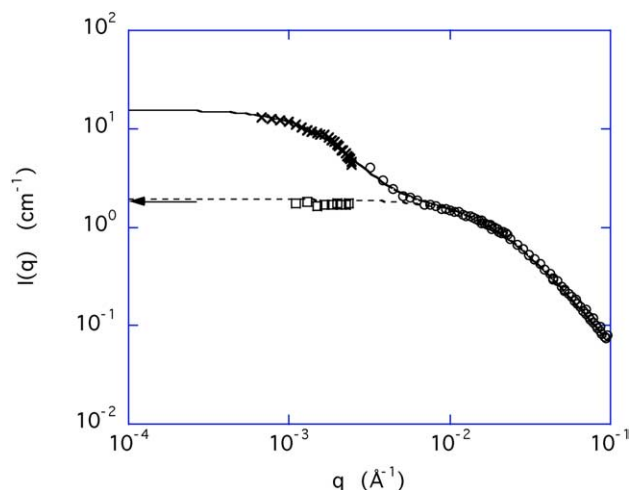


Fig. 2. SANS (open circles) and SLS (crosses) from a poly(vinyl alcohol) hydrogel at polymer concentration $\phi = 0.043$ with cross-link density 0.25%. Correlation lengths obtained from the fit to Eq. (1) are $\xi = 53$ Å and $\Xi = 425$ Å. Dashed line: first term of Eq. (1). Horizontal arrow: intensity estimated from macroscopic osmotic swelling pressure measurements (Eq. (7)) together with the corresponding neutron scattering contrast factor. Squares: intensity of osmotic fluctuations determined by DLS.

presence of structures of characteristic size 40–50 nm, which may be attributed to the microcrystallites. Since such molecular associations act as additional cross-links, they are expected to increase the value of the elastic shear modulus G . This expectation is verified by measurements of the shear modulus G as a function of the polymer volume fraction ϕ . Fig. 3 shows $G(\phi)$ for three different systems, of which two do not exhibit crystallization [polyacrylamide and poly(vinyl alcohol–vinyl acetate)]. The latter gel was prepared in a similar way to the PVA gel from a poly(vinyl alcohol–vinyl acetate) copolymer containing 12% (mole/mole) vinyl acetate co-monomer. In this sample, the randomly dis-

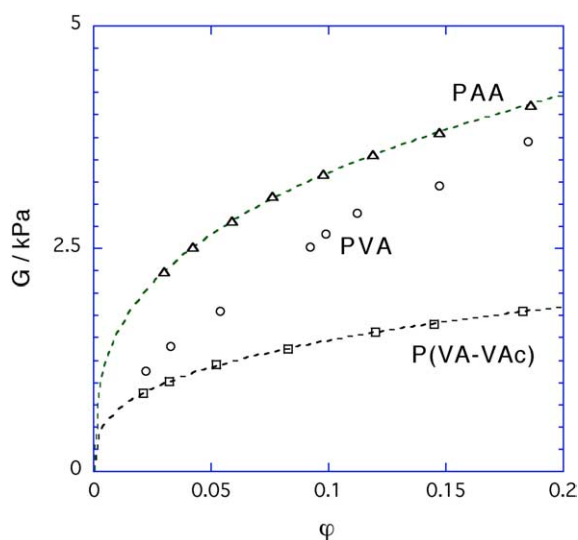


Fig. 3. Shear modulus G as a function of polymer volume fraction ϕ under deswelling for (a) polyacrylamide (triangles), (b) poly(vinyl alcohol) (circles) and (c) poly(vinyl alcohol–vinyl acetate) copolymer gels (squares).

tributed acetate groups severely limit hydrogen bonding and prevent crystallization. The dashed curve through the polyacrylamide data points is the fit to Eq. (8) with the parameter $G_0 = 7.5$ kPa and $m = 0.33 \pm 0.01$, while that for the copolymer is $G_0 = 3.1$ kPa and $m = 0.34 \pm 0.01$. For the polyvinyl alcohol gel, however, the observed exponent is higher (ca 0.6), indicating that the number of cross-links increases with increasing polymer concentration.

To understand the origin of the excess intensity at low q , measurements were also made on a uniaxially stretched sample. Fig. 4 shows a two-dimensional isointensity SANS pattern from a stretched PVA gel, swollen in D_2O . This experiment in principle provides a distinction between those features that are intrinsically isotropic, such as scattering from thermal fluctuations at high values of q (first term in Eq. (1)) and those that are related to the frozen-in elastic constraints. In the undeformed gel, the mutually interpenetrating crystalline domains form an isotropic percolating structure. When the gel matrix is stretched, the crystalline domains disinterpenetrate along the stretch axis. The density fluctuations in the stretch direction are enhanced, thus giving rise to the butterfly pattern of this figure.

4.2. Polyelectrolyte gel

Strongly charged polyelectrolytes in salt solutions might be expected to behave like uncharged polymers. Under physiological conditions, however, salt concentrations are relatively low and, in addition, specific ion binding may play a role, particularly if higher valence counter-ions are present. As the concentration of bivalent counterions increases, such gels are observed to undergo a volume

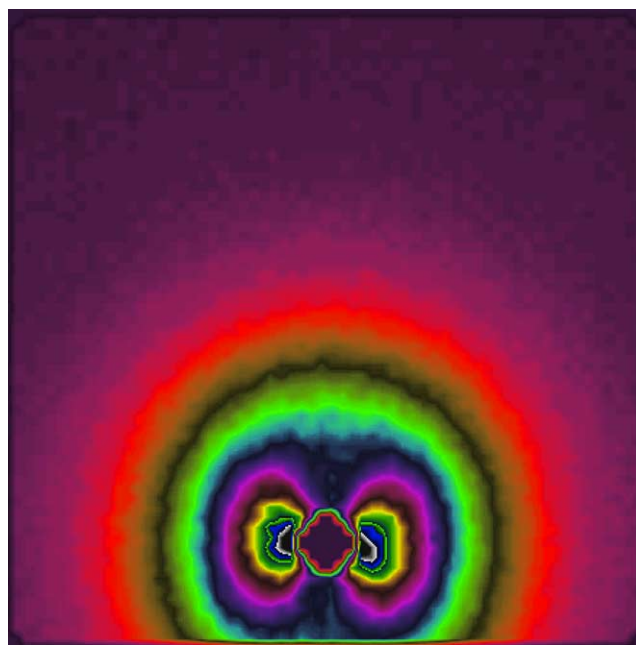


Fig. 4. SANS isointensity contour diagram for a stretched PVA gel (stretch ratio 1.5, $\phi = 0.37$); q -range of diagram ± 0.1 Å $^{-1}$.

transition from an expanded to a collapsed state. It is important to differentiate whether this volume transition is due to formation of additional cross-links through bridging of polyanions by divalent cations or to modification of the thermodynamic interactions in the polymer–solvent system. Fig. 5 shows the dependence of the shear modulus G of polyacrylate gels containing different amounts of calcium as a function of polymer volume fraction. The dashed curve is the fit to Eq. (8) with parameters $G_0=7.2$ kPa and $m=0.33\pm 0.01$. The evidence of Fig. 5 indicates that the contribution of the calcium ions to the elastic modulus is negligible.

Fig. 6 shows the SANS spectra of a polyacrylate gel in a solution of 40 mM NaCl with two different calcium contents, one below (0.6 mM CaCl_2) and one above (2.0 mM) the transition (1.0 mM CaCl_2). The principal features of these spectra are (1) at low q a power law behavior with a slope of approximately -3.6 , characteristic of a surface fractal; (2) an intermediate region of slope approximately -1 and (3) at higher q , a shoulder, similar to that found in neutral gels.

The shape of the curves in Fig. 6 is qualitatively different from that of the corresponding neutral polyacrylamide gel. The excess intensity at small q is caused by clustering of the polyelectrolyte chains, and is well documented in the literature [21]. The $\log I(q)$ vs. $\log q$ plot gives a straight line with a slope of approximately -3.6 . Such a power-law scattering is indicative of the fractal-like behavior of the system. For scattering from three-dimensional objects with fractal surface, the power law exponent is $-(6-D_s)$, where D_s is the fractal dimension of the surface ($2 < D_s < 3$). $D_s=2$ represents a smooth surface. The slope of the log–log plot in Fig. 6 yields a surface fractal dimension of $D_s=2.4$.

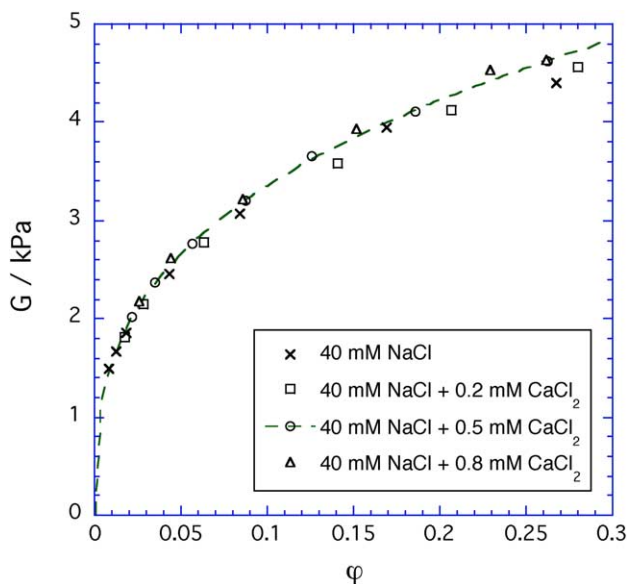


Fig. 5. Measured values of the shear modulus G of a sodium poly(acrylate) gel as a function of polymer volume fraction ϕ in 40 mM NaCl solution containing different amounts of CaCl_2 .

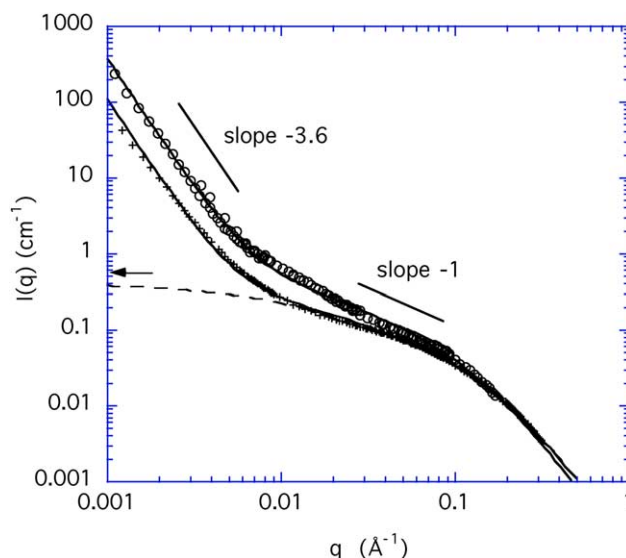


Fig. 6. SANS intensity from sodium sodium poly(acrylate) hydrogel in 40 mM NaCl solution with two different CaCl_2 concentrations (+0.6 mM CaCl_2 , \circ 2.0 mM CaCl_2). Lines: fit to Eq. (11) to data of 0.6 mM CaCl_2 sample, together with the osmotic component. Horizontal arrow: intensity estimated from macroscopic osmotic swelling pressure measurements (Eq. (7)) together with the corresponding neutron scattering contrast factor.

The Debye–Bueche term cannot account for the q^{-1} behavior in the intermediate q region, which is characteristic of a linear array of scattering centers. To describe this behavior, the following expression for the osmotic component is adopted [22],

$$I_{\text{osm}}(q) = \Delta\rho^2(\phi^2/M_{\text{os}})(1 + qL)^{-1}(1 + q^2\xi^2)^{-1} \quad (10)$$

where L is the persistence length of the polymer in the semi-dilute solution. For the low q feature in the SANS spectra a simple power law may be used, since, in the absence of a plateau, no correlation length can be attributed. The total expression used for fitting these spectra then becomes [22]

$$I(q) = A(1 + qL)^{-1}(1 + q^2\xi^2)^{-1} + Bq^{-n} \quad (11)$$

where the value of the exponent n for the present system is close to 3.6, and the quantities A , B , L and ξ are adjustable constants.

In Fig. 6 are also shown the fits of expression 11 to SANS spectra from the two samples. The dashed curve shows the osmotic component (Eq. (10)) of this fit to the data below the transition. The arrow on the left axis of the diagram is the intensity of the thermal fluctuations calculated from the osmotic swelling pressure and elastic modulus measurements. This estimate is meaningful only for the gel with the lower calcium concentration, i.e., below the volume transition. Above the transition, where the system loses its homogeneity, meaningful osmotic measurements could not be made. It is clear that the agreement between the data from the scattering and the macroscopic techniques is reasonable and that Eq. (11) reproduces the main features of the scattering curve.

5. Conclusions

Small angle neutron scattering measurements of various types of hydrogel are able to detect differences in the local organization of the polymer chains induced by interactions of different spatial ranges. In neutral gels, structural perturbations arising from the non-uniform distribution of cross-links generate excess scattering at small values of q . Although, the intensity scattered by these perturbations can be large, their contribution to the osmotic properties of the gel is negligible. In polyvinyl alcohol hydrogels, a secondary structure stabilized by hydrogen bonds is superimposed on to the underlying chemically cross-linked network. Moreover, an increase in the elastic modulus is observed, indicating that the main contribution from this structure is qualitatively similar to that arising from the chemical cross-links, namely frozen-in concentration fluctuations. The presence of the secondary superstructure does not modify the mechanism of the thermal fluctuations in these gels. The latter are described by an Ornstein–Zernike expression the amplitude of which is consistent with the osmotic modulus deduced from macroscopic osmotic and mechanical observations. These gels, when subjected to uniaxial strain, exhibit a butterfly scattering pattern, which results from the disinterspersion of mutually folded crystallites. The deformation of the gel produces no alteration in the Ornstein–Zernike component of the scattering signal, indicating that osmotic properties of the anisotropic gel at high q remain unchanged.

The scattering response of the polyelectrolyte gel is different from that of the neutral gels. At low q the poly(sodium acrylate) hydrogel in solution with excess salt displays power law behavior characteristic of a fractal surface, with a surface dimensionality close to $D_s = 2.4$. The lower bound of this region could not be resolved. At intermediate q the signal varies as q^{-1} , indicating that aligned regions of the polymer chain participate in the osmotic fluctuations. At higher q -values a shoulder is observed analogous to that in a neutral gel. The description required to fit the data involves a short length scale ξ , analogous to that in the Ornstein–Zernike expression, and a larger length scale L taking the form of a persistence length. Non-linear regression yields acceptable agreement with the result of independent macroscopic observations.

Acknowledgements

The authors acknowledge the support of the Institut Laue Langevin, Grenoble, France and the National Institute of Standards and Technology, US Department of Commerce in providing neutron research facilities used in this experiment. We are grateful both to Dr I. Grillo and Dr B. Hammouda for their invaluable help in these measurements. This work is based upon activities supported by the National Science Foundation under Agreement No. DMR-9986442.

References

- [1] Mark JE. *Adv Polym Sci* 1982;44:1–26.
- [2] Mark JE. *J Phys Chem B* 2003;107:903–13.
- [3] Horkay F, Hecht AM, Mallam S, Geissler E, Rennie AR. *Macromolecules* 1991;24:2896–902.
- [4] Mallam S, Horkay F, Hecht AM, Geissler E. *Macromolecules* 1989; 22:3356–61.
- [5] Horkay F, Burchard W, Geissler E, Hecht AM. *Macromolecules* 1993; 26:1296–303.
- [6] Schosseler F, Ilmain F, Candau SJ. *Macromolecules* 1991;24: 225–34.
- [7] Ricka J, Tanaka T. *Macromolecules* 1984;17:2916–21. *Macromolecules* 1985;18: 83–5.
- [8] Skuori R, Schosseler F, Munch JP, Candau SJ. *Macromolecules* 1995; 28:197–210.
- [9] Horkay F, Tasaki I, Bassar PJ. *Biomacromolecules* 2000;1:84–90.
- [10] Debye P, Bueche RM. *J Appl Phys* 1949;20:518–36.
- [11] Flory PJ. *Principles of polymer chemistry*. Ithaca, NY: Cornell University Press; 1953.
- [12] Tanaka T, Hocker LO, Benedek GB. *J Chem Phys* 1973;59:5151–6.
- [13] Treloar LRG. *The physics of rubber elasticity*. Oxford: Clarendon Press; 1976.
- [14] NIST Cold Neutron Research Facility. NG3 and NG7 30-meter SANS Instruments Data Acquisition Manual; January 1999.
- [15] Vink H. *Eur Polym J* 1971;7:1411–9.
- [16] Horkay F, Zrinyi M. *Macromolecules* 1982;15:1306–10.
- [17] Geissler E. In: Brown W, editor. *Dynamic light scattering. The method and some applications*. Oxford: Oxford University Press; 1993.
- [18] Ornstein LS, Zernike F. *Proc Sect Sci K Med Akad Wet* 1914;17:793.
- [19] de Gennes PG. *Scaling concepts in polymer physics*. Ithaca, NY: Cornell University Press; 1979.
- [20] Sears VF. *Neutron News* 1992;3:26.
- [21] Williams CE, Nierlich M, Cotton JP, Jannink G, Boue F, Daoud M, et al. *J Polym Sci, Polym Lett Ed* 1979;17:379–84.
- [22] Horkay F, Grillo I, Bassar PJ, Hecht AM, Geissler E. *J Chem Phys* 2002;117:9103–6.